Talanta 159 (2016) 401–411

Contents lists available at ScienceDirect

Talanta

journal homepage: www.elsevier.com/locate/talanta

Rapid and alternative fabrication method for microfluidic paper based analytical devices

Soheil Malekghasemi [a], Enver Kahveci [a,b], Memed Duman [a,*]

[a] Nanotechnology and Nanomedicine Division, Institute of Science, Hacettepe University, Ankara, Turkey
[b] UNAM-National Nanotechnology Research Center, Bilkent University, Ankara 06800, Turkey

ARTICLE INFO

Article history:
Received 11 March 2016
Received in revised form
15 June 2016
Accepted 20 June 2016
Available online 22 June 2016

Keywords:
Microfluidic paper based analytical device
Microwave irradiation
Point of care
Ink-jet printing
Silylation
Cellulose fibers

ABSTRACT

A major application of microfluidic paper-based analytical devices (μPADs) includes the field of point-of-care (POC) diagnostics. It is important for POC diagnostics to possess properties such as ease-of-use and low cost. However, μPADs need multiple instruments and fabrication steps. In this study, two different chemicals (Hexamethyldisilazane and Tetra-ethylorthosilicate) were used, and three different methods (heating, plasma treatment, and microwave irradiation) were compared to develop μPADs. Additionally, an inkjet-printing technique was used for generating a hydrophilic channel and printing certain chemical agents on different regions of a modified filter paper. A rapid and effective fabrication method to develop μPADs within 10 min was introduced using an inkjet-printing technique in conjunction with a microwave irradiation method. Environmental scanning electron microscope (ESEM) and x-ray photoelectron spectroscopy (XPS) were used for morphology characterization and determining the surface chemical compositions of the modified filter paper, respectively. Contact angle measurements were used to fulfill the hydrophobicity of the treated filter paper. The highest contact angle value ($141^\circ \pm 1$) was obtained using the microwave irradiation method over a period of 7 min, when the filter paper was modified by TEOS. Furthermore, by using this method, the XPS results of TEOS-modified filter paper revealed Si2p (23%) and Si-O bounds (81.55%) indicating the presence of Si–O–Si bridges and Si(OEt) groups, respectively. The ESEM results revealed changes in the porous structures of the papers and decreases in the pore sizes. Washburn assay measurements tested the efficiency of the generated hydrophilic channels in which similar water penetration rates were observed in the TEOS-modified filter paper and unmodified (plain) filter paper. The validation of the developed μPADs was performed by utilizing the rapid urease test as a model test system. The detection limit of the developed μPADs was measured as 1 unit ml^{-1} urease enzyme in detection zones within a period of 3 min. The study findings suggested that a combination of microwave irradiation with inkjet-printing technique could improve the fabrication method of μPADs, enabling faster production of μPADs that are easy to use and cost-effective with long shelf lives.

1. Introduction

Biosensors are used for early diagnosis, and they play a crucial role in preventing the progression of diseases [1]. Point-of-care (POC) diagnostics have attracted much attention as they improve health and treatment in resource-limited settings. POC diagnostics are preferred to other detection techniques owing to factors such as disposability, affordability, ease-of-use, and portability [2–4]. Recently, there is a widespread increase in the desire and willingness to use substances made from paper and paper-like (e.g., nitrocellulose membrane) materials for POC test systems, as paper and paper-like materials are inexpensive, plentiful, and degradable [5]. Among these systems, microfluidic paper-based analytical devices (μPADs) are extremely promising, as they are cost-effective, easy to operate, quick, precise, and sustainable over time and different environmental conditions [6,7].

The main fabrication concept of μPADs includes the separation of hydrophilic channels by hydrophobic walls. Several different approaches have been proposed in the literature for development of μPADs, including photolithography [8], wax dipping [9], flexographic printing [10], wax printing [11,12], plotting [13], plasma etching [14], wax screen-printing [15], and knife and laser cutting [16,17] technologies. However, these techniques have their own disadvantages. An obvious and common limitation of these methods is the difficulty regarding the deposition of biological and chemical reagents in the final form of the test system [18]. Additionally, photolithography and wax dipping methods require multiple processing steps, sophisticated and expensive

* Corresponding author.
E-mail address: memi@hacettepe.edu.tr (M. Duman).

http://dx.doi.org/10.1016/j.talanta.2016.06.040
0039-9140/

instruments, and are not suitable for mass production. Bruzewicz et al. [13] used the plotting technique and Polydimethylsiloxane (PDMS) as a hydrophobization agent to generate a microfluidic pattern. The main disadvantages of this method include the complex determination of the appropriate viscosity of dissolved PDMS in hexanes, the resolution quality of hydrophobic barrier, and the long curing period of PDMS. The drawback of wax printing involves multiple fabrications steps such as the printing of wax on paper by a wax printer, heating the paper in an oven, and printing reagents on a test zone by inkjet printing. Moreover, the wax is unevenly spread on the paper, thereby lowering the resolution quality. Another disadvantage of this technique is the lack of proper facilities for printed reagents in wax printer [11,12]. Li et al. [19] used Alkenyl ketene dimer and Alkyl ketene as hydrophobic agents and n-heptane as a solvent to prepare a solution. As n-Heptane is highly flammable, it can be explosive when its vapor mixes with air. Given these factors, it could be argued that n-Heptane is harmful for printer parts and especially for cartridges. Wang et al. also fabricated paper-based microfluidic device by using harmless inorganic solvent (1 M NaOH) as an etching agent. In this study NaOH etched the methylsilsesquioxane (MSQ) modified paper and the performances of this procedure was compared to wax and alkylketene dimer (AKD)-modified filter paper's procedure [20].

Among printing technologies, the ink-jet printing technique possesses several advantages over the previously discussed fabrication methods. The main advantages of this technology are high pattern precision and resolution, the rapid printing of multiple pages, low cost, reproducibility, and the ability to work with very small volumes of ink (picolitres) [21]. In addition, inkjet printers were modified to fabricate multianalyte chemical sensing paper [22], print DNA chips [23], and cell patterns [24].

The above-mentioned reasons clearly indicate that there is still a strong need for new fabrication approaches with high reproducibility, fast manufacturing time, cost effectiveness, safety, simplicity, and ease of use.

This study presents a cheap, rapid, and easy fabrication method for μPADs based on chemical pattering by microwave irradiation and inkjet-printing. Hydrophobization of paper was achieved and compared using two different chemicals (Hexamethyldisilazane (HMDS) and Tetraethylorthosilicate (TEOS)), which were irradiated by a kitchen type microwave device. Moreover, other common methods, such as normal heating and plasma treatment, were tested in order to compare the silanization efficiency in microwave irradiation. Furthermore, developed μPADs were adapted to the rapid urease test as a proof of concept by spotting related biomolecules into detection zones using an inkjet printer. This new and rapid fabricating method had several obvious advantages given the low number of process steps, cost-effectiveness, and fabrication of the μPADs within the shortest time span (~10 min).

2. Materials and methods

2.1. Chemicals and materials

Whatman® qualitative filter paper, Grade 4, was obtained from Sigma-Aldrich with a thickness and pore size of 205 μm and 20–24 μm, respectively. HMDS (98%) was obtained from Alfa Aesar. TEOS (99%), and hydrochloric acid (HCl 37%) were obtained from Merck. Distilled and deionized water was used for all aqueous sample and dilutions. 50 mM urea solution (pH 5.5) containing 1.5 g urea (Sigma-Aldrich), 6.5 mg phenolsulfonphthalein (PSP) as an indicator, 20 mg citric acid (Acros Organics N.V.), and 30 mg Sodium phosphate (Sigma-Aldrich) was used. Urease solution (pH 6.0) was prepared by using a mixture of urease (4000 units g^{-1}, Jack Bean Urease from Sigma-Aldrich) in 0.1 M potassium phosphate buffer.

2.2. Hydrophobization of filter paper

In order to hydrophobize the filter paper, two different silylating agents HMDS and TEOS were selected and their silylation efficiencies were compared by environmental scanning electron microscopy (ESEM), x-ray photoelectron spectroscopy (XPS), and water contact angle (WCA) measurements. Diluted hydrochloric acid (HCl) was also used as a catalyst when the HMDS was used as a silylating agent. The hydrophobization of filter paper was mainly achieved by microwave (kitchen type) irradiation. Moreover, two different common methods (heating and plasma treatment) were also selected and used to compare the efficiency of microwave irradiation.

2.2.1. Silylation of filter paper cellulose with HMDS

The HMDS solution was prepared by a mixture of HMDS and 1 M HCl in a mole-ratio of 9:1 to hydrophobize the filter paper (1 cm × 1 cm). Three different methods were used for the silylation of paper cellulose. In the heating method, filter paper was dipped in a glass beaker containing both HMDS and 1 M HCl mixture. The beaker was placed in a water bath at 80 °C for 2 h, 4 h, 8 h, 16 h, and 24 h. Plasma treatment (Vacuum Praha, Czech Republic with a 13.56 MHz radio frequency generator) was used to deposit HMDS-HCl (1 M) solution as a monomer on filter paper. This procedure was performed at RF power levels of 50 W and 100 W for 10 min and 15 min in each power level. In the microwave irradiation method, filter papers were soaked in HMDS-HCl (1 M) solution, and were then processed in a kitchen type microwave oven (0.65–0.7 kW) for 5 min and 10 min. The chemical analysis of the surface of hydrophobized paper was performed using x-ray photoelectron spectroscopy (XPS, Thermo-K-Alpha-Monochromated high-performance XPS Spectrometer) in which a Al K-Alpha source gun was operated at 1.4 kV focus voltage, 6 mA beam current, and 400 μm spot size. An environmental scanning electron microscope (ESEM-FEI Quanta 200 FEG) was used to examine the morphology of treated filter papers. The hydrophobicity of the treated filter paper was also performed using WCA measurements (DSA100, Krüss Gmbh) at room temperature.

2.2.2. Silylation of filter paper cellulose with TEOS

TEOS was selected as an alternative silylation agent instead of HMDS. In this case, the same three methods (heating, plasma treatment, and microwave irradiation) were used to create a hydrophobic layer on filter paper. In the heating method, filter paper was treated with a heated TEOS solution (80 °C) for 2 h, 4 h, 8 h, 16 h, and 24 h in a water bath. In the plasma treatment, the silylation of cellulose fibers by TEOS was achieved at RF power levels of 50 W and 100 W for 10 min, 15 min, and 30 min. In the microwave irradiation method, filter paper was immersed in a TEOS solution and irradiated by microwave at 0.65–0.7 kW for 5 min and 7 min. The silylation efficiencies of the cellulose fibers were also characterized using XPS, ESEM and WCA measurements.

2.3. Generation of microfluidic channels on filter paper

Hydrophilic channels on the modified filter paper were generated by two different approaches. In the case of the first one, the inkjet printer (HP- Deskjet 670C) was used to apply different concentrations of HCl solution (0.001–1 M) to etch a hydrophobic layer on the paper. Multiple etching cycles were performed (printing cycles are 3 times), and the regeneration of the native hydrophilic characteristics of cellulose fibers was compared by XPS, ESEM, WCA, and Washburn assay measurements.

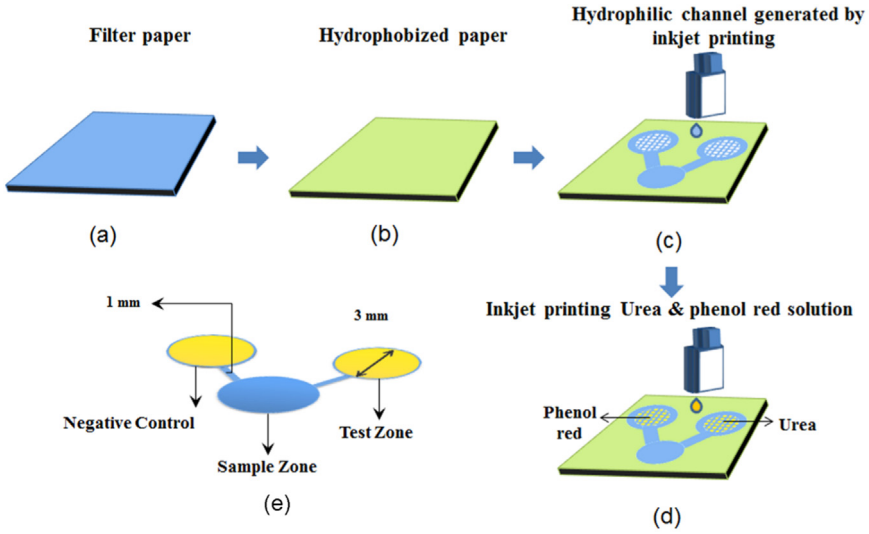

Scheme 1. Fabrication steps of the paper-based rapid urease test. (a) Plain filter paper, (b) a hydrophobic layer originating from HMDS and TEOS precursors, (c) an etching modified filter paper by inkjet printing technique to form hydrophilic channels, (d) a urea-phenol red mixture and phenol red solution printed on the test zone and negative control zone, respectively, (e) the size and the names of different zones and channels in the V-shaped paper-based device.

Furthermore, a second alternative approach was also used to create a hydrophilic channel on the paper. First, the inverse of the desired pattern was printed with 1 M HCl on native hydrophilic (unmodified) filter paper that was later immersed in a HMDS solution (without HCl catalyst). Following this, the paper was treated by microwave irradiation for 5 min and 10 min and it was characterized with XPS, ESEM, and WCA measurements.

2.4. Fabrication of paper-based rapid urease test by using inkjet printing on μPAD

A V-shaped paper-based rapid urease test consisting of two channels and three zones (sample, test, and control), was patterned by inkjet printing in a single step. The hydrophilic channels were generated using the first approach as described above. The biological reagents, which was used for urease test, were filled into 2 reservoirs of HP-49 Tri-color cartridge. A urea and phenol red mixture, filled in the first reservoir of this cartridge, was spotted on the test zone. Additionally, the second reservoir of cartridge, filled with only a phenol red solution, was ejected to the control zone simultaneously (Scheme 1c and d). 0.03 μl of the each reagent (printing cycles are 10 times) from both reservoirs was printed on test and control zones of the paper-based rapid urease test. The pattern of the V shape of the μPAD was sketched using Microsoft Power Point software. The channel width was 1000 μm and the deposition zone diameter was 3000 μm (Scheme 1e).

In order to validate and reveal the detection limit of the developed μPAD, 5 μl artificial urease sample solution (1–20 units ml^{-1}) was applied onto the sample zone. The color change at the test zones was observed by naked eye and a digital camera captured images to determine the response time of the test kit. Furthermore, quantitative analytical response of the test system was analyzed using color intensity measurements, done by ImageJ program.

3. Results and discussion

3.1. Silylation of cellulose with HMDS

In order to create the hydrophobic barrier on the filter paper, two different chemicals (HMDS and TEOS) were used as silylating agents.

One of the main reagents, HMDS, was used to prepare trimethylsilyl cellulose (TMSC) since the 1950s [25]. Various catalysts (mostly acidic, such as HCl) and heating should be used to increase the silylation efficiency of HMDS [26,27]. The silylation reactions of the cellulose fibers of the filter paper with HMDS were summarized in Scheme 2a. Briefly, the presence of HCl in the HMDS solution allowed the conversion of HMDS to chlorotrimethylsilane (TMSCL), which was more reactive than the HMDS. Following this, the TMSCL reacted with the hydroxyl group of cellulose. Ammonia and hydrochloric acid, which were defined as by-products, could leave the reaction mixture when the reaction reached completion [27,28]. According to studies on the silanization chemistry of cellulose with HMDS, 2 mol HMDS per mole OH function was used to achieved the best silylation yield [27].

Cold plasma processing is the second method that is widely used for the deposition of organosilicon (e.g. TEOS and HMDS) compounds. Plasma can create ions, free radicals, and other reactive species by using free energetic electrons [29]. The energetic electrons cause the dissociation of HMDS to precursors such as Si–N–Si bonds and Si–(CH_3)x (X=1, 2, 3) to create –Si–CH_2–Si–(CH_3)x (X=1,2,3) bonds. The presence of CH_3 groups on the modified filter paper showed hydrophobic characteristics following the chemical reaction [29,30].

As a novel method, applied in this study, Trimethylsilyl groups were detached from the HMDS and were grown on the cellulose by microwave irradiation at atmospheric conditions. The HMDS was exposed to 0.67–0.7 kW of microwave radiation and allowed to chemisorb trimethylsilyl groups on –OH groups of the cellulose. As a result of this reaction, cellulose–O–$Si(CH_3)_3$ groups were formed, and NH_3 remained as a by-product [31,32].

3.2. Silylation of cellulose with TEOS

Because of its lower toxicity when compared to another silane precursor, TEOS is the precursor for deposition on various substrates [33]. Moreover, as the silicon atom in TEOS is already oxidized, alkoxysilanes have deposit potentials without oxygen sources [34]. By using the three stated methods to create a single film on filter paper, the ethoxy groups in TEOS bonded with –OH groups of cellulose, and the polarity of the filter paper changed

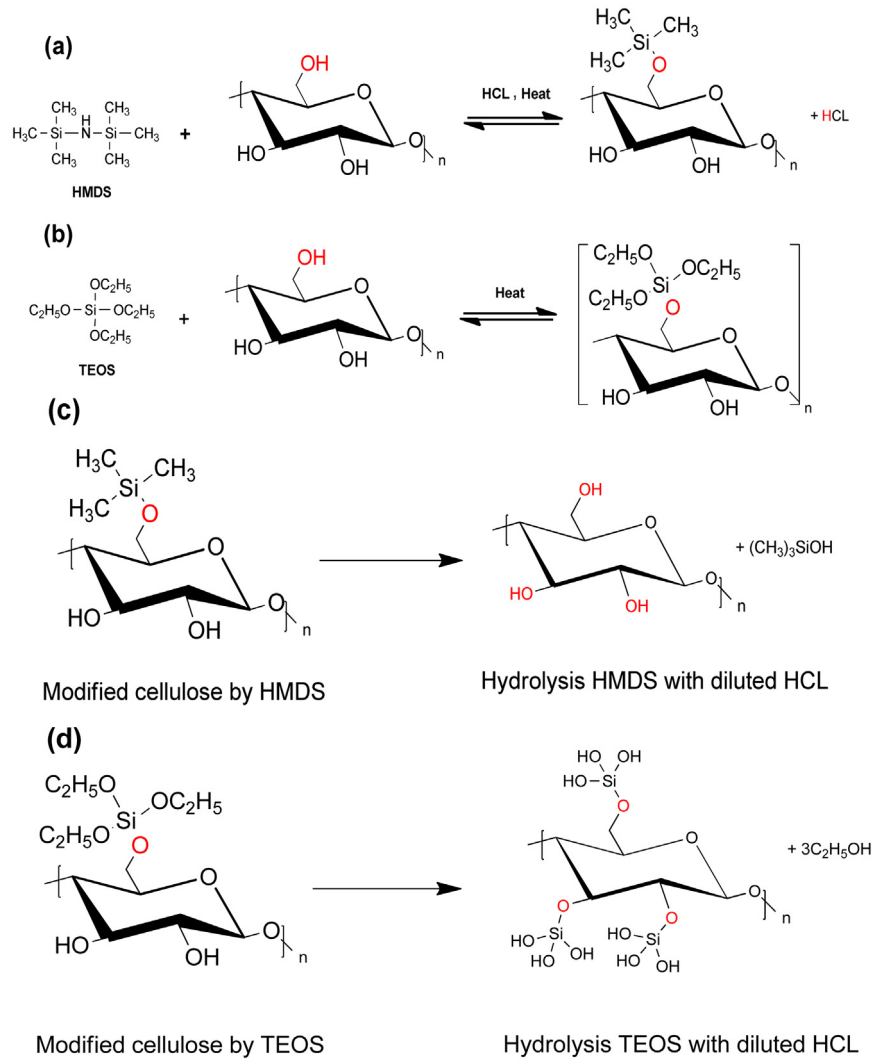

Scheme 2. Reactions causing the silylation and desilylation of the cellulose fibers. (a) Reaction between the HMDS-HCl solution and the cellulose fibers of the filter paper. (b) The reaction of the TEOS molecules with the cellulose fibers of the filter paper. (c) Hydrolysis of the HMDS-modified filter paper by diluted HCl. (d) Hydrolysis of the TEOS-modified filter paper by diluted HCl.

from hydrophilic to hydrophobic.

The sol-gel process at a low temperature was used to hydrophobize the filter paper in the heating method. Moisture in the environment contributed to the hydrolysis of alkoxysilanes such that the ethoxy ligands decomposed by the scission of the O–C bond. After that, the reaction occurred through the condensation of alkoxysilanes, and led to Si–O–Si bridge formation on the celluloses. The temperature and duration of the reaction had to be adjusted well, as the ethoxysilane species (formed from the dissociation of the TEOS) could be further decomposed and converted to hydrophilic SiO_2 film [35].

Additionally, TEOS is a common reagent that contributed to film deposition processing by cold plasma. The dissociation of the TEOS occurred because of the high amount of energetic electrons in an oxygen-free atmosphere. This caused the TEOS molecules to be transferred into small fragments of ethoxysilane species [34]. The oxygen atoms of cellulose showed a strong affinity to silicon atoms of ethoxysilane species. Hence, a cellulose–O–Si–O structure was formed on the filter paper by the adsorption of these small fragments to the –OH groups of cellulose [29,36].

In this study, the hydrophobization of the filter paper was also achieved by microwave irradiation in which the thermal decomposition of TEOS occurred. Surface topography was altered when the TEOS was exposed to the sample at 0.65–0.7 kW. At this temperature, the bonds between O and C broke and led to the decomposition of ethoxy functional groups. Tri and diethoxysiloxanes and a Si–O–Si network were formed during the reaction. Thus, the hydrophobization of the filter paper was established through the interaction with the hydroxyl groups of cellulose [37–39].

3.3. Water contact angle (WCA) measurements

Water contact angle measurements comprised the first and simple characterization method to prove the silylation of modified filter paper. The highest contact angle values in dependence of treatment methods and time are summarized in Table 1.

In the case of the HMDS+HCl modification, the optimal hydrophobic surface (WCA: $140° \pm 2$) was achieved by plasma treatment in which the paper was treated with HMDS+HCl mixture as a monomer solution at 100 W for 15 min (Table 1). When shorter treatment time (10 min) were applied at 100 W RF power, the WCA values were measured at approximately $118° \pm 3$. Furthermore, a lower RF power (50 W) was not sufficient to modify the filter paper (WCA $< 35.4° \pm 4$).

In the second modification method (heating), the filter paper

Table 1
Water contact angle values on the modified paper.

Procedure	Reagents for modification	Water contact angle (deg.)	Time
Heating	HMDS+HCL	127 ± 6	4 (h)
	TEOS	145 ± 1	24 (h)
Plasma	HMDS+HCL	140 ± 2	10 (min)
	TEOS	120 ± 2	30 (min)
Microwave	HMDS+HCL	107 ± 3	10 (min)
	Printed HCL+ HMDS	124 ± 4	10 (min)
	TEOS	141 ± 1	7 (min)

was incubated with a HMDS+HCl mixture at 80 °C for 2 h, 4 h, 8 h, 16 h, and 24 h. While the lowest silylation yield was observed at 2 h (suggesting that the reaction time was not sufficient to create hydrophobic properties for the filter paper), the highest WCA (127° ± 6) were measured at 4 h (Table 1). The further extension of the incubation time did not significantly change the hydrophobization efficiency (WCAs were 118° ± 9, 116° ± 5, 123° ± 8 for 8 h, 16 h, and 24 h, respectively).

Plasma treatment and heating methods require complex equipment and longer reaction times, respectively. Thus, microwave irradiation was applied as the last and the new method to provide a simpler and quicker modification of the filter paper. However, highest WCA value (107° ± 3) obtained when the paper treated at the highest power (0.7 kW) for 10 min (Table 1). Additionally, a second alternative method was also used to modify the filter paper as described in the generation of the microfluidic channel on the filter paper in the experimental section. In this method, the highest WCA value measured was 124° ± 4 at 0.7 kW RF power for 10 min (Table 1).

The WCA measurements were also applied to the TEOS modified paper, which was prepared by the same three methods. In the plasma treatment methods, the filter paper was exposed to TEOS monomers at different RF powers (50 W and 100 W) and times (10 min, 15 min, and 30 min). The highest WCA value (120° ± 2) was measured at maximum conditions (100 W, 30 min) as shown in Table 1.

When the paper samples were incubated with TEOS for 2 h and 4 h at 80 °C in the heating method, it was observed that they still retained their hydrophilic properties. Longer incubation times were associated with higher WCA values (the WCAs were 120° ± 7 and 130° ± 3 for 8 h and 16 h, respectively). The best hydrophobic surface (WCA: 145° ± 1) was achieved by the heating method at 80 °C for 24 h (Table 1).

In the case of the last modification method (MW irradiation), the highest WCA values (141° ± 1) were obtained when the paper samples were modified at 0.7 kW (the maximum RF power) for 7 min.

3.4. X-ray photoelectron spectroscopy (XPS) measurements

XPS was performed to determine the silylation of the cellulose fiber in the filter paper. Table 2 shows the measured values for the filter papers, which were modified by two different silylating agents (HMDS and TEOS) and three different modification methods (heating, plasma treatment, and microwave irradiation). Further, the corresponding data of unmodified paper was also placed in Table 2 to compare silylation procedures.

3.4.1. XPS measurements on HMDS modified filter paper

The binding of $Si(Me)_3$ groups to the –OH groups of the cellulose (Scheme 2a), produced by the HMDS-HCl mixture, showed two typical peaks with binding energies of 100 eV and 150 eV, corresponding to Si2p and Si2s, respectively. These peaks indicated the presence of the Si element on the surface of the hydrophobized paper. Furthermore, the C–Si bond, which appeared at approximately 283 eV, proved the existence of Si(Me)x groups on the filter paper. The best degree of silylation was achieved in the plasma treatment method at 100 W for 10 min. While the highest percentage of atomic concentration of C–Si was 59.9 in the plasma treatment, it was 16.88 in the heating method in which the filter paper was incubated at 80 °C for 4 h (Table 2).

In the plasma treatment, since the system under the vacuum condition, an oxynitride type film can be formed in filter paper during polymerization of HMDS. Therefore, there was a corresponding peak of N molecule in the XPS analysis data. However, in the heating and the microwave irradiation methods, N molecules can easily evaporate during the reaction in the form of ammonia (by-products) from the open system [27,28].

In the microwave irradiation, two different approaches were used for the modification of the filter paper with the HMDS. The characteristic peaks of Si2p, Si2s, and C–Si were also observed in these two methods (Fig. 1a and b). According to Table 2, these two approaches generated equal silylation in terms of the atomic concentration of C–Si at 0.7 kW for 10 min.

3.4.2. XPS measurements on TEOS modified filter paper

Because of the dissociation of TEOS by using heating energy, RF power (plasma deposition system), and electromagnetic radiation (microwave oven), Si(OEt) groups were detected on celluloses of filter paper by XPS analysis [40]. These groups reacted with –OH groups of cellulose and created a hydrophobic barrier (Scheme 2b).

When heating and plasma methods were applied, the percentages of the measured Si-O compositions were 62.41 and 37.59, respectively (Table 3). These results indicated that the Si–O–Si-$(OEt)_x$ (x=1,2,3) hydrophobic film was successfully formed. The atomic concentration and the composition of other elements are also shown in Table 2. The maximum atomic concentration of Si,

Table 2
XPS analysis of the filter paper deposited with different silylating agents and different procedures.

Procedure	Sample	Atomic concentration (%)				Composition of atomic concentration (%)			
		Si	O	C	N	C–H, C–C	C–Si	C–O	O–C–O, C=O
Unmodified Paper		–	43.83	56.17	–	7.81	–	62.52	29.67
Heating	HMDS+HCl	3.99	37.19	58.28	–	3.07	16.88	62.64	17.41
	TEOS	15.3	40.27	44.44	–	58.17	–	37.88	3.95
Plasma	HMDS+HCl	21.56	12.19	56.95	9.31	27.28	59.9	10.42	2.4
	TEOS	7.49	25.63	63.41	–	51.16	–	45.08	3.76
Microwave	HMDS+HCl	2.42	40.62	56.96	–	3.51	12.25	60	24.24
	Printed HCl+ HMDS	2.1	40.9	57	–	3.13	8.52	64.63	23.72
	TEOS	23	49.95	27.05	–	46.54	–	14.99	38.47

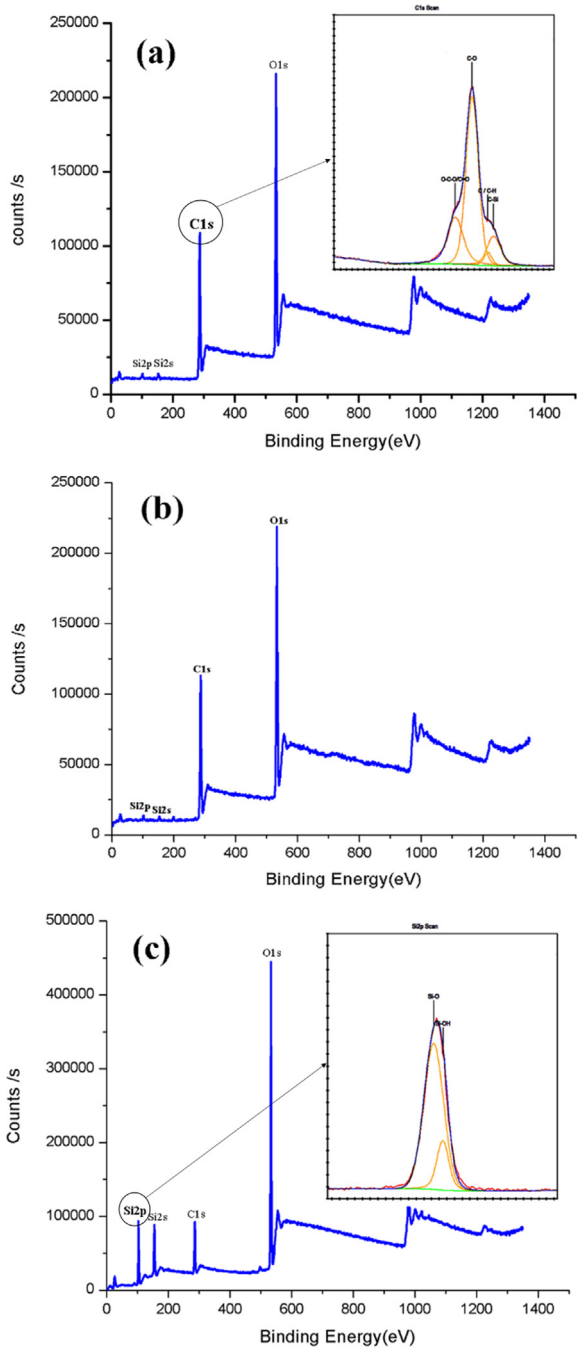

Fig. 1. XPS measurement of the filter paper (a) modified by HMDS- HCL, (b) printed by HCL and then modified by HMDS and (c) modified by TEOS through microwave irradiation.

23, was achieved in microwave irradiation, while using TEOS as a precursor.

The thermal decomposition of TEOS to siloxanes occurred immediately, when the filter paper was treated with neat TEOS under microwave irradiation. The existence of Si2p (Fig. 1c) and the higher amount of Si–O relative to the Si–OH bonds (Table 3) indicated the presence of Si–O–Si bridges and Si(OEt) groups on the modified filter paper, respectively.

Atomic concentration of Si elements, C–Si and Si–O bonds were the factors that made native paper become different from modified paper in the case of hydrophobization. When these factors were analyzed and compared with the modified ones, no any corresponding values were measured in native paper (Table 2). These findings were also proved that the hydrophobic functional groups had been placed on the cellulose fibers.

3.5. Morphology of paper surface with ESEM

ESEM was also used to investigate the morphology of the HMDS and TEOS treated filter papers, which were developed by microwave irradiation. Prior to scanning the modified paper, the unmodified filter paper was analyzed and the analysis revealed cellulose fibers with a pore size of approximately 20–25 μm (Fig. 2a). In the first approach of HMDS modification method, the filter paper was treated just with the HMDS-HCl mixture. A Si–O–Si network coating is clearly observed in Fig. 2b.

The inkjet printing technique was also used for ejecting diluted HCl on the paper surface in the second approach. Following this, the paper, treated with the HMDS, was immediately placed under microwave irradiation. A thin layer of methyl groups was also coated between the cellulose fibers (Fig. 2d). In both modification approaches, the porous structures of the papers were changed, and the fiber matrix interface was clearly observed, as suggested by the decrease in the pore sizes.

In the case of the TEOS modification method, electromagnetic radiation in the microwave spectrum caused the generation of thermal energy causing the spread of the TEOS over the paper surface. The formation of Si–O–Si networks was clearly observed with decreasing pore sizes of the cellulose fiber (Fig. 2f).

3.6. Generation of hydrophilic channels

Various concentrations of diluted HCl–H_2O (0.001–1 M) solutions were used to hydrate and generate the hydrophilic channels by acid-catalyzed hydrolysis mechanisms [41,42]. $H3O^+$ and Cl^- were produced when the diluted HCl was applied to the HMDS modified papers. This reaction detached the $-(CH_3)_3Si$ groups and produced the $(Me_3)_3SiOH$ (Trimethylsilanol) (Scheme 2c) [43]. As a result of this reaction, the hydrophobized filter paper returned to its initial form (Fig. 2c and e). The effect of the diluted HCl on the TEOS modified hydrophobic paper could be summarized as the

Table 3
XPS results of the modified filter paper before and after hydrolysis.

Procedure	Sample	Composition of atomic concentration (%)							
		C–H		C–Si		Si–O		Si–OH	
		Before	After	Before	After	Before	After	Before	After
Heating	HMDS+HCl	3.07	31.36	16.88	–	–	–	–	–
	TEOS	–	–	–	–	62.41	34.36	37.59	65.64
Plasma	HMDS+HCl	27.28	75.52	59.9	–	–	–	–	–
	TEOS	–	–	–	–	93.72	56.52	6.28	43.48
Microwave	HMDS+HCl	3.51	14.24	12.25	–	–	–	–	–
	Printed HCl+ HMDS	3.13	15.08	8.52	–	–	–	–	–
	TEOS	–	–	–	–	81.55	37.94	18.45	62.06

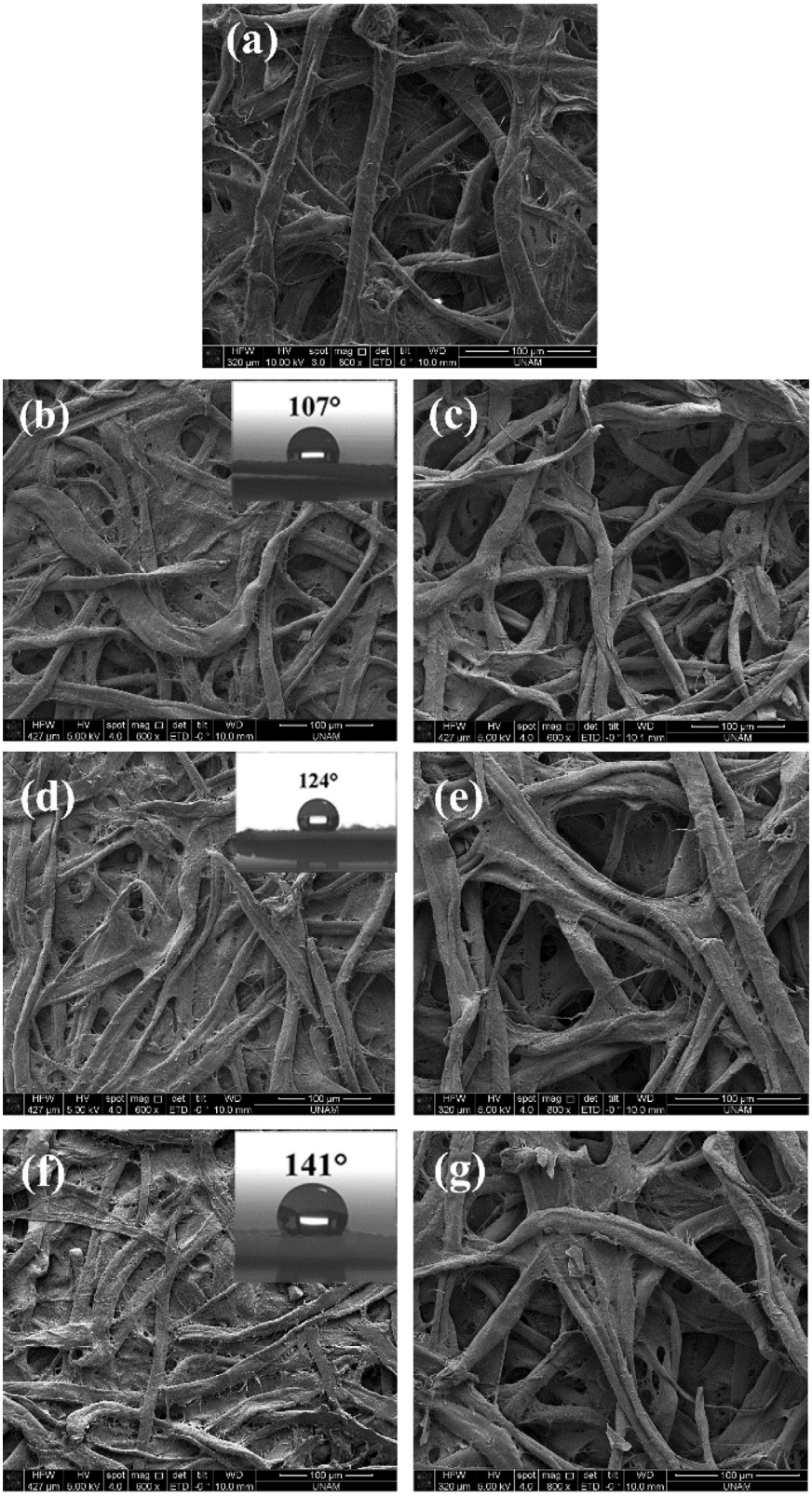

Fig. 2. SEM images of (a) unmodified filter paper. (b) Modified filter paper by the HMDS-HCl mixture. (c) HCl-etching of the modified filter paper in the (b) section. (d) Modified filter paper printed by HCl and then treated with HMDS. (e) HCl-etching of the modified filter paper in the (c) section. (f) Modified filter paper by TEOS. (g) HCl-etching of the modified filter paper in the (f) section. All modified filter papers in this figure were prepared by the microwave irradiation method. Scale bar is 100 μm for each images.

detachment of $-C_2H_5$ groups from the modified paper and the formation of C_2H_5OH (Ethanol) as by-products (Scheme 2d) [44]. When the TEOS modified paper was hydrolyzed by the diluted HCl, Si–OH bounds formed and the previously formed network disappeared as observed in the ESEM image (Fig. 2g).

Table 3 shows the XPS results after the hydrolysis of the treated

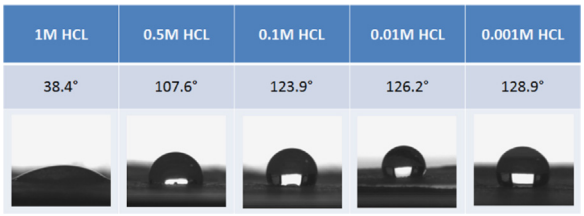

Fig. 3. WCA pictures and values of the modified filter paper treated with different concentrations of HCl.

paper with 1 M HCl. Both the disappearance of C–Si bonds on the HMDS modified paper samples and the increase in the Si–OH bonds on the TEOS modified paper samples served as proofs of the generation of hydrophilic channels.

The effect of different HCl concentrations on the wetting properties of the modified paper was also analyzed by water contact angle measurements (Fig. 3). The highest WCA value was 128.9° when the modified paper was treated with 0.001 M HCl solution. However, adequate levels of the hydrophilic property were achieved with 1 M HCl solution.

In order to demonstrate the performance of the developed patterning method, channels with various widths were generated on modified filter paper by printing technique (Fig. 4a). The channels with 2 and 1 mm widths were achieved by three printing cycles, while the channels with 0.1 and 0.01 mm widths were generated by six printing cycles. However, if the printing cycle is applied more than four times, the sharpness of the channel's wall was destroyed. This can be explained by penetration of excess etching agents (diluted HCl) around the channel's wall. After examining the optimum widths and different printing cycles to generate the best working channel, 1 mm width size with three printing cycles was chosen for fabrication of rapid urease test. The minimum achievable width of flow channels under these parameters was attained as 0.67 mm (Fig. 4b).

The depth of etching through the paper was also analyzed and showed the full penetration of dye solution within the cross-section of the hydrophilic channel (Fig. 4c). Moreover, the resistance of the hydrophobic barriers, formed by TEOS, against different surfactants and organic solvents were also investigated (Fig. 4d). According to these findings, the barriers cannot stand a long time when they are exposed to alcohols (Methanol and Isopropanol), surfactants (Triton X-100 and Sodium dodecyl sulfate (SDS)), and toluene. However, they showed very good resistance to dimethyl sulfoxide (DMSO).

3.7. *Liquid penetration behavior by using Washburn equation*

The performance of the generated hydrophilic channels was studied by common Washburn assay (Fig. 5a). In this experimental set up, hydrophilic channels were generated by inkjet printing method as describe above on TEOS modified papers. The liquid penetration behavior of these generated channels were compared to both the same sized plain (unmodified) filter paper (W4-

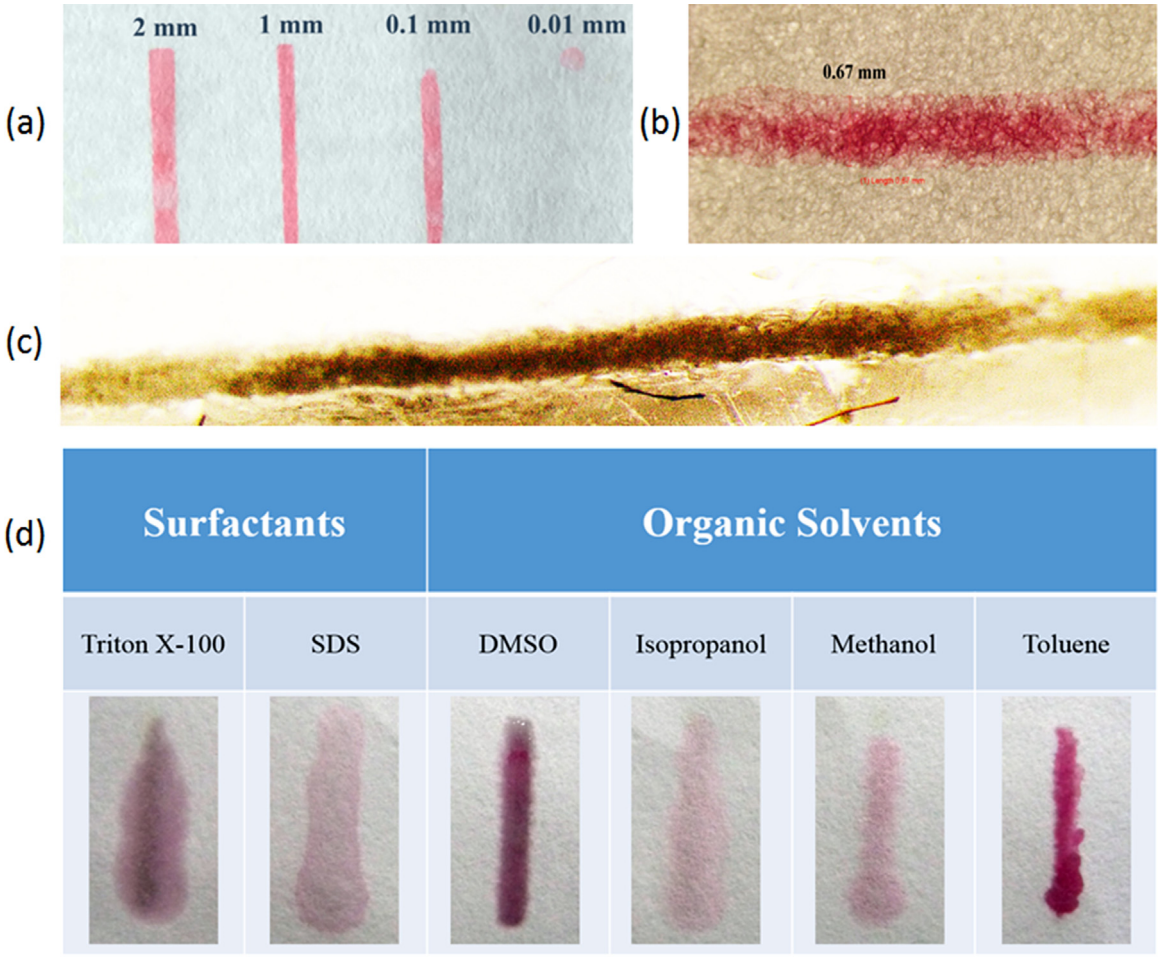

Fig. 4. The assessment of the developed patterning method. (a) Four channels with various widths (2, 1, 0.1, and 0.01 mm). (b) Minimum reachable width of flow channel (0.67 mm). (c) The cross-section image of the hydrophilic channel; the black region of the image shows penetration of dye. (d) The resistance of the hydrophobic barriers when they are exposed different surfactants and organic solvents.

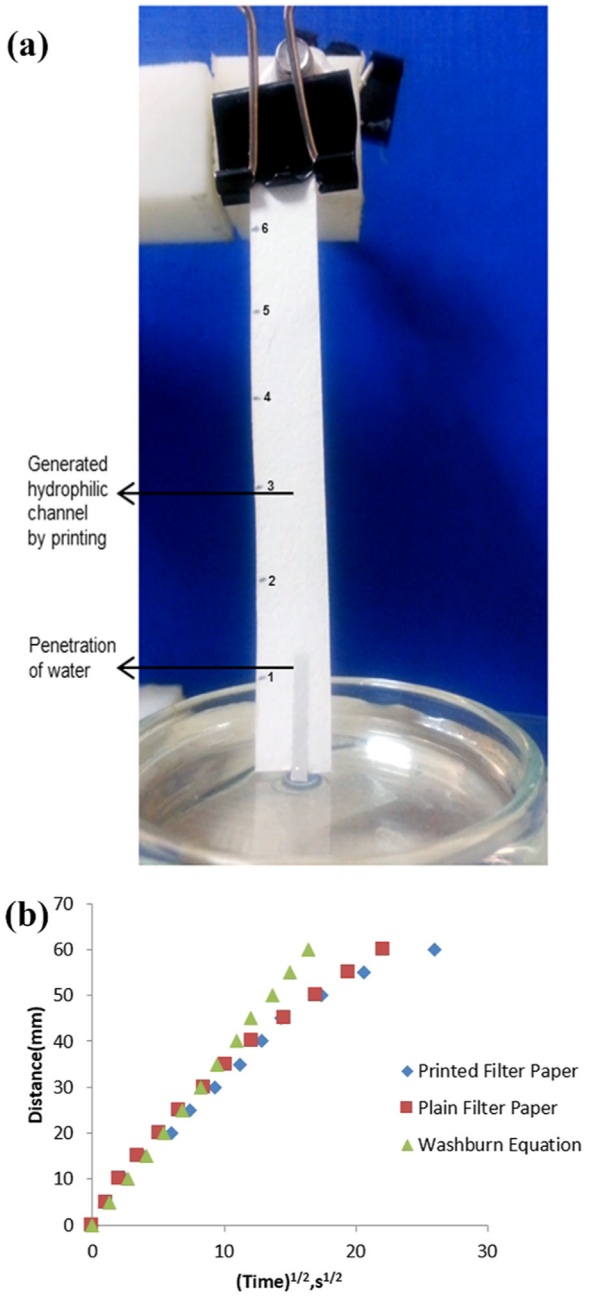

Fig. 5. (a) Experimental setup of water penetration studies on modified filter paper, and (b) a comparison of water penetration distances for printed filter paper, plain filter paper, and solid lines derived from the Washburn equation as a function of the square root of time.

Whatman 4) and the Washburn equation (Eq. (1)) that yielded the first order approximation of liquids in the paper [45].

$$l^2 = \gamma r t \cos\theta / 2\eta \quad (1)$$

Where l is the distance traveled by the liquid, t is the time, r is the equivalent capillary pore radius of the paper, γ and η are the surface tension and viscosity of the liquid, respectively, and θ is the contact angle.

Water penetration rates between the printed hydrophilic channel (regenerated) and the plain filter paper were measured using a ruler, a timer, and a camera. The results indicated that the penetration profile in both paper channels were in perfect agreement (Fig. 5b). However, it should be noted that there was a slight deviation between the linear lines, which come from experimental data and Washburn equation after 10 s. A few explanations may account for this deviation. First, the fiber swelling resulting in the loss of the driving force at longer penetration times is the most likely cause of the deviation. Second, the Washburn model did not consider the gravity factor, and thus, the deviation could also be affected by the gravity factor [19].

3.8. Colorimetric detection of Helicobacter pylori by paper-based rapid urease test

A rapid urease test is based on the activity of the urease enzyme, which is produced by the *Helicobacter pylori*, and dissociates urea into ammonia and carbon dioxide. Hence, the formation of ammonia increases the pH and can be detected by the indicator phenol red, which changes its color from yellow to magenta [46].

In order to test the developed microfluidic paper based analytical device (μPAD), a rapid urease test was used as a model test system. The urease enzyme (5 μl) was introduced as a sample to the μPAD to mimic the gel based rapid urease test. The developed V-shaped test system consisting of 2 channels and 3 zones (sample (S), test (T), control (C)) is shown in Fig. 6a.

A V-shaped test system indicates positive result when the yellow color in the T-zone turns to magenta (Fig. 6b). Fig. 6c shows the reaction between the urease solution (1 unit ml^{-1}) and the printed urea-phenol red mixture with respect to time. As seen in the figure, an observable color change started exactly after 3rd min and the color changed to magenta in 10 min. Additionally, the detection limit of developed μPAD system was also investigated by using different concentrations of the urease solution (Fig. 6d).

By considering the above-mentioned assay, the detectable limit of the developed μPAD by naked eye was found as low as 1 unit ml^{-1} urease enzyme. This limit is one order of magnitude lower than the common CLO test [47].

The performance of the developed μPAD was also analyzed by measuring color intensity, which also gives more quantitative results. Various units of urease enzyme were applied in five microliters to T-zone of the μPAD and color change was recorded. The color intensity was also measured and analyzed by ImageJ software. Fig. 7 is the quantitative analytical curve, which shows variation of the color intensity with different urease concentration (1–20 Units ml^{-1}). As seen in the calibration curve in Fig. 7, good linearity was obtained with a determination coefficient (R^2) around 0.98. Moreover, the detection limit of the sensor, calculated by dividing the three times of standard deviation of the color intensity of the blank to the slope of the linear calibration curve, was found as 0.50 units of enzyme.

4. Conclusion

This study demonstrates a combination of an inkjet printing technique and microwave irradiation that provides the rapid fabrication of a μPAD and allows the fast detection of urease activity. The combination of these two techniques resulted in the low cost of final products without using photoresist agent, or applying any curing steps, cutting methods and high temperature. Hydrophilic channels were generated with only one printing step, and then the urea and phenol red mixture was deposited on the modified filter paper. Furthermore, resistive hydrophobic barriers could be easily obtained by the microwave treatment within minutes (~7 min), instead of using longer heating process or complicated plasma treatment. In the last part of the study, μPAD was developed as rapid urease test to quantify its limit of detection and to test its response time. According to experimental findings, this device can sense as low as 0.5 units of urease enzyme with in 3 min.

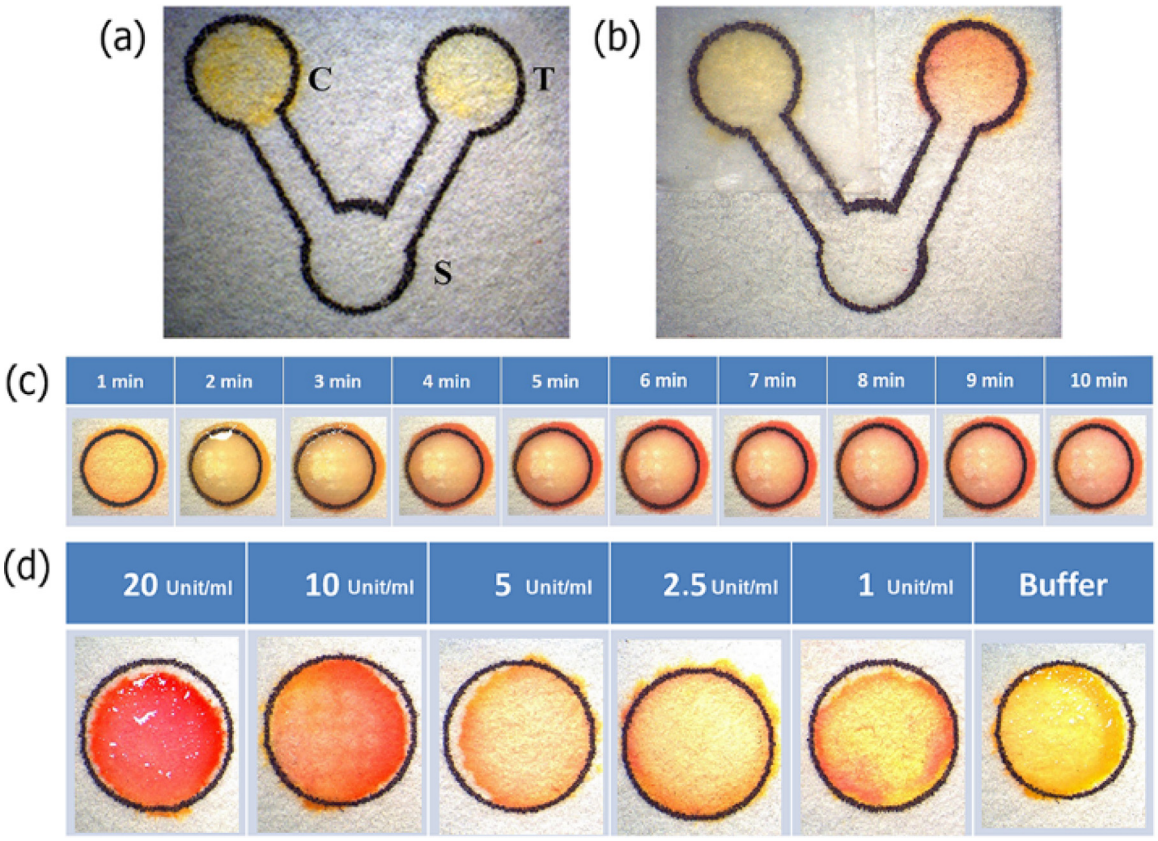

Fig. 6. (a) V-shaped rapid urease test system fabricated by the inkjet printing technique. (b) Tested V-shaped system with the observable color change. The color change (c) over time via a reaction between the urease solution and urea-phenol red mixture and (d) with respect to the different concentrations of the urease solution.

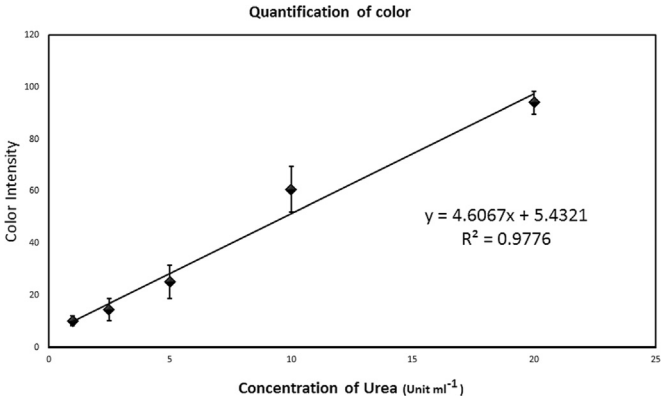

Fig. 7. Colorimetric response of developed μPAD against different concentration of urease enzymes.

In summary, the new and rapid fabrication method proposed in this study is simple and straightforward. Hence, it can be used to develop more advanced paper-based devices for the detection of biologically relevant samples such as organic pollutants, pathogens, toxins, drug residues, and vitamins.

Acknowledgements

This work was financially supported by TUBITAK (The Scientific and Technological Research Council of Turkey) with the project number of 1003–113S076.

References

[1] M.M. Ali, S.D. Aguirre, Y. Xu, C.D.M. Filipe, R. Pelton, Y. Li, Detection of DNA using bioactive paper strips, Chem. Commun. (2009) 6640–6642.
[2] P. Yager, G.J. Domingo, J. Gerdes, Point-of-care diagnostics for global health, Annu. Rev. Biomed. Eng. 10 (2008) 107–144.
[3] W.G. Lee, Y.-G. Kim, B.G. Chung, U. Demirci, A. Khademhosseini, Nano/Microfluidics for diagnosis of infectious diseases in developing countries, Adv. Drug Deliv. Rev. 62 (2010) 449–457.
[4] V. Gubala, L.F. Harris, A.J. Ricco, M.X. Tan, D.E. Williams, Point of care diagnostics: status and future, Anal. Chem. 84 (2012) 487–515.
[5] P. von Lode, Point-of-care immunotesting: approaching the analytical performance of central laboratory methods, Clin. Biochem. 38 (2005) 591–606.
[6] W. Zhao, A. van der Berg, Lab on paper, Lab Chip 8 (2008) 1988–1991.
[7] C. Parolo, A. Merkoçi, Paper-based nanobiosensors for diagnostics, Chem. Soc. Rev. 42 (2013) 450–457.
[8] A.W. Martinez, S.T. Phillips, M.J. Butte, G.M. Whitesides, Patterned paper as a platform for inexpensive, low-volume, portable bioassays, Angew. Chem. Int. Ed. 46 (2007) 1318–1320.
[9] T. Songjaroen, W. Dungchai, O. Chailapakul, W. Laiwattanapaisal, Novel, simple and low-cost alternative method for fabrication of paper-based microfluidics by wax dipping, Talanta 85 (2011) 2587–2593.
[10] J. Olkkonen, K. Lehtinen, T. Erho, Flexographically printed fluidic structures in paper, Anal. Chem. 82 (2010) 10246–10250.
[11] E. Carrilho, A.W. Martinez, G.M. Whitesides, Understanding wax printing: a simple micropatterning process for paper-based microfluidics, Anal. Chem. 81 (2009) 7091–7095.
[12] Y. Lu, W. Shi, L. Jiang, J. Qin, B. Lin, Rapid prototyping of paper-based microfluidics with wax for low-cost, portable bioassay, Electrophoresis 30 (2009) 1497–1500.
[13] D.A. Bruzewicz, M. Reches, G.M. Whitesides, Low-cost printing of poly(dimethylsiloxane) barriers to define microchannels in paper, Anal. Chem. 80 (2008) 3387–3392.
[14] X. Li, J. Tian, T. Nguyen, W. Shen, Paper-based microfluidic devices by plasma treatment, Anal. Chem. 80 (2008) 9131–9134.
[15] W. Dungchai, O. Chailapakul, C.S. Henry, A low-cost, simple, and rapid fabrication method for paper-based microfluidics using wax screen-printing, Analyst 136 (2011) 77–82.
[16] E.M. Fenton, M.R. Mascarenas, G.P. López, S.S. Sibbett, Multiplex lateral-flow test strips fabricated by two-dimensional shaping, ACS Appl. Mater. Interfaces 1 (2009) 124–129.

[17] E. Fu, B. Lutz, P. Kauffman, P. Yager, Controlled reagent transport in disposable 2D paper networks, Lab Chip 10 (2010) 918–920.
[18] K. Maejima, S. Tomikawa, K. Suzuki, D. Citterio, Inkjet printing: an integrated and green chemical approach to microfluidic paper-based analytical devices, RSC Adv. 3 (2013) 9258.
[19] X. Li, J. Tian, G. Garnier, W. Shen, Fabrication of paper-based microfluidic sensors by printing, Colloids Surf. B Biointerfaces 76 (2010) 564–570.
[20] J. Wang, R.N. Monton, X. Zhang, C.D.M. Filipe, R. Pelton, M.R.N. Monton, et al., Hydrophobic sol-gel channel patterning strategies for paper-based microfluidics, Lab Chip 14 (2014) 691–695.
[21] L. Setti, A. Fraleoni-Morgera, B. Ballarin, A. Filippini, D. Frascaro, C. Piana, An amperometric glucose biosensor prototype fabricated by thermal inkjet printing, Biosens. Bioelectron. (2005) 2019–2026.
[22] K. Abe, K. Suzuki, D. Citterio, Inkjet-printed microfluidic multianalyte chemical sensing paper, Anal. Chem. 80 (2008) 6928–6934.
[23] T. Okamoto, T. Suzuki, N. Yamamoto, Microarray fabrication with covalent attachment of DNA using bubble jet technology, Nat. Biotechnol. 18 (2000) 438–441.
[24] E.A. Roth, T. Xu, M. Das, C. Gregory, J.J. Hickman, T. Boland, Inkjet printing for high-throughput cell patterning, Biomaterials 25 (2004) 3707–3715.
[25] A.E. Pierce, Silylation of Organic Compounds: A Technique for Gasphase Analysis, Pierce Chemical Company, Rockford, 1968.
[26] J. Nagy, A. Borbély-Kuszmann, K. Becker-Pálossy, E. Zimonyi-Hegedüs, Über den lösungsmitteleffekt bei der silylierung von cellulose mit hexamethyldisilazan, Die Makromol. Chemie. 165 (1973) 335–338.
[27] C. Nouvel, P. Dubois, E. Dellacherie, J.-L. Six, Silylation reaction of dextran: effect of experimental conditions on silylation yield, regioselectivity, and chemical stability of silylated dextrans, Biomacromolecules 4 (2003) 1443–1450.
[28] C.P. Tripp, M.L. Hair, Reaction of chloromethylsilanes with silica: a low-frequency infrared study, Langmuir 7 (1991) 923–927.
[29] I.H. Tan, M.L.P. da Silva, N.R. Demarquette, Paper surface modification by plasma deposition of double layers of organic silicon compounds, J. Mater. Chem. 11 (2001) 1019–1025.
[30] M.L.P. da Silva, I.H. Tan, A.P. Nascimento Filho, E. Galeazzo, D.P. Jesus, Use of plasma polymerized highly hydrophobic hexamethyldissilazane (HMDS) films for sensor development, Sens. Actuators B Chem. 91 (2003) 362–369.
[31] M. Lindblad, A. Root, Preparation of Catalysts VII, in: Proceedings of the 7th International Symposium on Scientific Bases for the Preparation of Heterogeneous Catalysts, Elsevier, 1998.
[32] S.D. Bhagat, Y.-H. Kim, G. Yi, Y.-S. Ahn, J.-G. Yeo, Y.-T. Choi, Mesoporous SiO_2 powders with high specific surface area by microwave drying of hydrogels: a facile synthesis, Microporous Mesoporous Mater. 108 (2008) 333–339.
[33] A. Pecora, L. Maiolo, G. Fortunato, C. Caligiore, A comparative analysis of silicon dioxide films deposited by ECR-PECVD, TEOS-PECVD and Vapox-APCVD, J. Non Cryst. Solids 352 (2006) 1430–1433.
[34] M. Abbasi-Firouzjah, S.-I. Hosseini, M. Shariat, B. Shokri, The effect of TEOS plasma parameters on the silicon dioxide deposition mechanisms, J. Non Cryst. Solids 368 (2013) 86–92.
[35] P.C.A. Jerónimo, A.N. Araújo, M. Conceição, B.S.M. Montenegro, Optical sensors and biosensors based on sol-gel films, Talanta 72 (2007) 13–27.
[36] M.T. Kim, Deposition kinetics of silicon dioxide from tetraethylorthosilicate by PECVD, Thin Solid Films 360 (2000) 60–68.
[37] J. Spitzmüller, J. Braun, H. Rauscher, R.J. Behm, Dissociative adsorption and site specificity in the initial stages of tetraethoxysilane (TEOS) interaction with Si (111)-(7 × 7), Surf. Sci. 400 (1998) 356–366.
[38] J. Spitzmüller, J. Braun, H. Rauscher, R.J. Behm, Thermal decomposition of tetraethoxysilane (TEOS) on Si(111)-(7 × 7), Appl. Phys. A 66 (1998) 1021–1024.
[39] N. Primeau, C. Vautey, M. Langlet, The effect of thermal annealing on aerosol-gel deposited SiO_2 films: a FTIR deconvolution study, Thin Solid Films 310 (1997) 47–56.
[40] L.L. Tedder, G. Lu, J.E. Crowell, Mechanistic studies of dielectric thin film growth by low pressure chemical vapor deposition: The reaction of tetraethoxysilane with SiO_2 surfaces, J. Appl. Phys. 69 (1991) 7037.
[41] D.A. Donatti, A.I. Ruiz, D.R. Vollet, A dissolution and reaction modeling for hydrolysis of TEOS in heterogeneous TEOS-water-HCl mixtures under ultrasound stimulation, Ultrason. Sonochem. 9 (2002) 133–138.
[42] G.K. Cooper, K.R. Sandberg, J.F. Hinck, Trimethylsilyl cellulose as precursor to regenerated cellulose fiber, J. Appl. Polym. Sci. 26 (1981) 3827–3836.
[43] E. Kontturi, P.C. Thüne, J.W. (Hans) Niemantsverdriet, Cellulose model surfaces simplified preparation by spin coating and characterization by x-ray photoelectron spectroscopy, infrared spectroscopy, and atomic force microscopy, Langmuir 19 (2003) 5735–5741.
[44] C.C. Egger, M.W. Anderson, G.J.T. Tiddy, J.L. Casci, In situ NMR and XRD studies of the growth mechanism of SBA-1, Phys. Chem. Chem. Phys. 7 (2005) 1845.
[45] K.T. Hodgson, J.C. Berg, The effect of surfactants on wicking flow in fiber networks, J. Colloid Interface Sci. 121 (1988) 22–31.
[46] C. Ricci, J. Holton, D. Vaira, Diagnosis of *Helicobacter pylori*: invasive and non-invasive tests, Best. Pract. Res. Clin. Gastroenterol. 21 (2007) 299–313.
[47] T. Sato, M.A. Fujino, Y. Kojima, F. Kitahara, T. Nakamura, K. Kubo, et al., 4708 Immunological rapid urease test-a new diagnostic system for detecting *Helicobacter pylori*, Gastrointest. Endosc. 51 (2000) AB209.